

FIRST REDSHIFT DETERMINATION OF AN OPTICALLY/ULTRAVIOLET FAINT SUBMILLIMETER GALAXY USING CO EMISSION LINES

A. WEIß¹, R. J. IVISON^{2,3}, D. DOWNES⁴, F. WALTER⁵, M. CIRASUOLO^{2,3}, AND K. M. MENTEN¹

¹ Max-Planck Institut für Radioastronomie, Auf dem Hügel 69, 53121 Bonn, Germany

² UK Astronomy Technology Centre, Royal Observatory, Blackford Hill, Edinburgh, EH9 3HJ, UK

³ Institute for Astronomy, University of Edinburgh, Royal Observatory, Blackford Hill, Edinburgh, EH9 3HJ, UK

⁴ Institut de Radio Astronomie Millimétrique, 300 Rue de la Piscine, Domaine Universitaire, 38406 Saint Martin d'Hères, France

⁵ MPIA, Königstuhl 17, 69117 Heidelberg, Germany

Received 2009 August 18; accepted 2009 September 15; published 2009 October 12

ABSTRACT

We report the redshift of a distant, highly obscured submillimeter galaxy (SMG), based entirely on the detection of its CO line emission. We have used the newly commissioned Eight Mixer Receiver at the IRAM 30 m telescope, with its 8 GHz of instantaneous dual-polarization bandwidth, to search the 3 mm atmospheric window for CO emission from SMM J14009+0252, a bright SMG detected in SCUBA Lens Survey. A detection of the CO(3–2) line in the 3 mm window was confirmed via observations of CO(5–4) in the 2 mm window. Both lines constrain the redshift of SMM J14009+0252 to $z = 2.9344$, with high precision ($\delta z = 2 \times 10^{-4}$). Such observations will become routine in determining redshifts in the era of ALMA.

Key words: cosmology: observations – galaxies: evolution – galaxies: high-redshift – galaxies: starburst – ISM: molecules

1. INTRODUCTION

Sensitive blank-field millimeter and submillimeter continuum surveys have discovered hundreds of dusty, star-forming submillimeter galaxies (SMGs) over the past decade (e.g., Smail et al. 1997; Barger et al. 1999; Borys et al. 2003; Greve et al. 2004; Coppin et al. 2006). Determining their redshift distribution has been much slower, however, because the large dust content of SMGs means that they often have only weak (if any) counterparts in the rest-frame ultraviolet and optical, making spectroscopic redshift determinations extremely difficult (e.g., Smail et al. 2002; Dannerbauer et al. 2002). Furthermore, the poor spatial resolution of millimeter/submillimeter continuum surveys (typically 11–19") means that several potential, faint optical/near-IR counterparts exist. This requires deep radio or *Spitzer* mid-IR images to pinpoint the most likely counterpart for optical spectroscopic follow-up observations (e.g., Ivison et al. 2002, 2004). The largest SMG redshift survey published so far was based on radio-identified SMGs (Chapman et al. 2005), which may bias the redshift distribution since radio emission may remain undetected even in the deepest radio maps for sources at $z > 3$.

A promising alternative route to determine the redshift of an SMG is through observations of CO emission lines at centimeter or millimeter wavelengths. These lines arise from the molecular gas, the fuel for star formation, and can thus be related unambiguously to the submillimeter continuum source. Therefore, these observations do not require any additional multi-wavelength identification and circumvent many of the problems inherent to optical spectroscopy of SMGs.

The narrow bandwidth of existing millimeter receivers, however, placed severe limitations on this approach as it was too time consuming to search blindly for the CO lines in redshift space via multiple frequency tunings. In recent years, much effort has been invested in overcoming this bandwidth limitation at various radio facilities (e.g., Naylor et al. 2003; Erickson et al. 2007; Harris et al. 2007). With the commissioning of the multi-band heterodyne receiver, Eight Mixer Receiver (EMIR), at the IRAM 30 m telescope, this situation has greatly improved.

EMIR's 8 GHz instantaneous, dual-polarization bandwidth in the 3 mm band provides the same spectral coverage as ALMA. Combined with the large collecting area of the 30 m telescope this allows for blind searches for high-redshift CO lines at millimeter wavelengths.

To demonstrate the capabilities of EMIR as a "redshift machine," we targeted SMM J14009+0252. This source was discovered by the SCUBA in early 1998 and is one of the brightest SMGs discovered to date ($S_{850 \mu\text{m}} = 15.6 \text{ mJy}$; Ivison et al. 2000). Despite several attempts, and the availability of an accurate radio position, no spectroscopic redshift could be determined—mainly because of its faintness at near-IR/optical wavelengths. In this Letter, we report the results of our blind search for CO lines in this SMG.

2. OBSERVING STRATEGY

The 3 mm (E090) setup of EMIR provides 8 GHz of instantaneous, dual-polarization bandwidth. The entire accessible frequency range, 83–117 GHz, can be covered with five tunings. This corresponds to $0 < z < 0.4$ for CO(1–0) and $1.0 < z < 8.7$ for the CO lines between ($J = 2 - 1$) and (7–6), with only a small gap at $1.78 < z < 1.98$. The gap can be covered by 2 mm observations, i.e., EMIR is a powerful instrument to search for high-redshift ($z > 1$) CO emission.

Observations were made in 2009 July during average summer conditions ($\sim 7 \text{ mm}$ precipitable water vapor). Data were recorded using 16 units of the Wideband Line Multiple Autocorrelator (WILMA, 1 GHz of bandwidth each) to cover 8 GHz in both polarizations. WILMA provides a spectral resolution of 2 MHz which corresponds to $5\text{--}7 \text{ km s}^{-1}$ for the 3 mm band. The observations were done in wobbler-switching mode, with a switching frequency of 1 Hz and an azimuthal wobbler throw of $100''$. Pointing was checked frequently on the nearby quasar J1226+023 and was found to be stable to within $3''$. Calibration was done every 12 minutes using the standard hot/cold-load absorber. The data were processed with the CLASS software. We omitted scans with distorted baselines and subtracted only linear baselines from individual spectra.

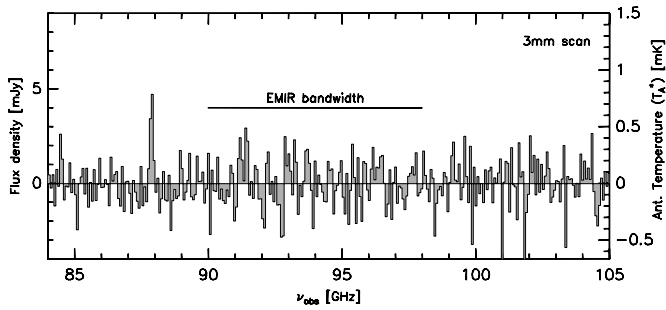


Figure 1. 20 GHz wide spectral scan at a velocity resolution of 200 km s^{-1} toward SMM J14009+0252 in the 3 mm window. A CO emission feature is seen at $\sim 88 \text{ GHz}$ (see Figure 2 for a presentation of the CO line at higher spectral resolution).

We first scanned the full 3 mm tuning range of EMIR with ~ 2 hr of observing for each tuning. The tunings were spaced to provide 500 MHz overlap. Excellent receiver noise temperatures across the band (35–45 K) resulted in typical system temperatures of $\sim 100 \text{ K}$. The resulting spectrum had an rms noise level of 0.5 mK ($\approx 3.5 \text{ mJy}$) at a velocity resolution of 200 km s^{-1} but did not show clear evidence for CO line emission. We then increased the integration time for the lower part ($< 105 \text{ GHz}$) of the 3 mm band until we reached an average rms noise level of 0.2 mK (1.2 mJy). The resulting spectrum, as shown in Figure 1, shows a line at $\sim 88 \text{ GHz}$.

At this stage, the source redshift was still not determined as it was not clear which CO transition was detected in the 3 mm scan. We therefore used the dual-frequency 3/2 mm (E090/E150) setup of EMIR to search for a second CO transition in the 2 mm band and to increase the signal-to-noise ratio (S/N) of the 3 mm line. In this configuration, each frequency band has an instantaneous, dual-polarization bandwidth of 4 GHz. The 2 mm mixers were tuned to 146.5 GHz , under the assumption that the 3 mm line was the CO(3–2) transition at $z = 2.93$. At this frequency, the receiver noise temperature was $\sim 30 \text{ K}$, yielding a system temperature of $\sim 120 \text{ K}$. SMM J14009+0252 was observed in the dual-frequency setup for $\sim 5 \text{ hr}$ and we clearly detected a second line in the 2 mm band (see Figure 2). Additional 2 mm data were taken in an attempt to observe a third

CO line in the 1 mm band (E150/E230 configuration). Given the relatively poor observing conditions, the 1 mm data did not yield a meaningful limit.

The beam sizes/antenna gains for the line frequencies at 3 and 2 mm are $28''/6.0 \text{ Jy K}^{-1}$ and $15''/6.5 \text{ Jy K}^{-1}$, respectively. We estimate the flux density scale to be accurate to $\pm 10\%$ – 15% .

3. RESULTS

The final 3 and 2 mm spectra are shown at a velocity resolution of 60 km s^{-1} in Figure 2. The rms noise level (T_A^*) for both spectra is $160 \mu\text{K}$ (1.0 mJy) and $180 \mu\text{K}$ (1.3 mJy) at 3 mm and 2 mm, respectively. Both lines are detected at high significance (9 and 12σ for the integrated intensities). The line profiles for both lines are very similar and well described by a single Gaussian with a FWHM of 470 km s^{-1} . The parameters derived from Gaussian fits to both line profiles are given in Table 1. The frequencies unambiguously identify the lines as CO(3–2) and CO(5–4) (see our discussion below). Combining the centroids of both lines, we derive a variance-weighted mean redshift for SMM J14009+0252 of $z = 2.9344 \pm 2 \times 10^{-4}$.

4. DISCUSSION

At first glance, the observed frequencies cannot only be interpreted as CO(3–2) and CO(5–4) at $z = 2.93$ but also as CO(6–5) and CO(10–9) at $z = 6.88$ or even CO(9–8) and CO(15–14) at $z = 10.80$. The CO ladder, however, is not equidistant in frequency which results in small, but significant differences for the frequency separation of the line pairs as a function of rotational quantum number. The frequency separation is 58.577 , 58.532 , and 58.458 GHz for the CO line pairs at redshifts 2.93, 6.88, and 10.80, respectively. Our observations yield $\delta\nu = 58.581 \pm 0.017 \text{ GHz}$, which identifies the lines as CO(3–2) and CO(5–4) at $z = 2.93$. Our redshift confirms earlier photometric redshift estimates by Ivison et al. (2000, $z > 2.8$ based on S_{450}/S_{850} and $3 < z < 5$ based on the whole spectral energy distribution (SED)), Yun & Carilli (2002, $z \sim 3.5$ based on the dust SED) and more recently by Hempel et al. (2008, $z = 2.8$ – 3 based on optical/IR photometry).

With the precise redshift and the observed CO line luminosities in hand, we can estimate the molecular gas content of

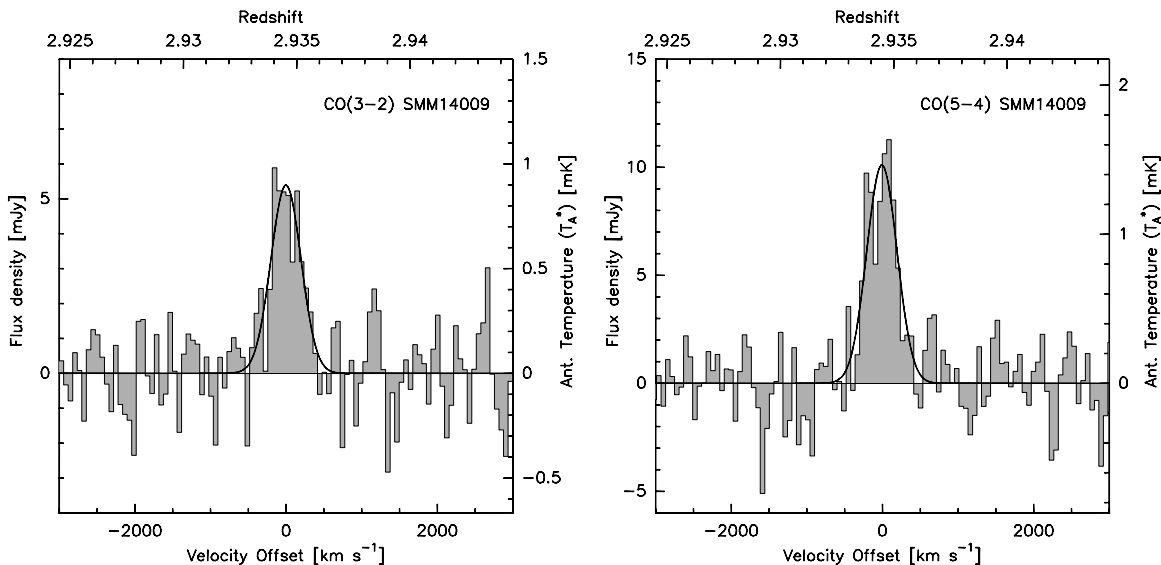


Figure 2. Spectra of the CO(3–2) (left) and CO(5–4) (right) lines toward SMM J14009+0252. The spectral resolution is 60 km s^{-1} for both lines. See Table 1 for the fit parameters.

Table 1
CO Line Parameters for SMM J14009+0252

Line	ν_{obs} (GHz)	z_{CO}	S_{ν} (mJy)	ΔV (km s ⁻¹)	I (Jy km s ⁻¹)	$L'^{\text{a,b}}$ (10 ¹⁰ K km s ⁻¹ pc ²)	$L^{\text{a,b}}$ (10 ⁷ L_{\odot})
CO(3–2)	87.888(8)	2.93450(35)	5.4 ± 0.9	470 ± 60	2.7 ± 0.3	7.9 ± 0.9	10.4 ± 1.2
CO(5–4)	146.469(9)	2.93438(26)	10.2 ± 1.3	472 ± 45	5.1 ± 0.4	5.3 ± 0.4	32.7 ± 2.7

Notes.

^a Corrected for a lens magnification of $m = 1.5$ (Ivison et al. 2000).

^b Adopted luminosity distance: 25.16 Gpc; angular size distance: 1.625 Gpc; linear scale: 7.879 kpc/'' (for $H_0 = 71$ km s⁻¹ Mpc⁻¹, $\Omega_{\Lambda} = 0.73$, and $\Omega_M = 0.27$ (Spergel et al. 2003)).

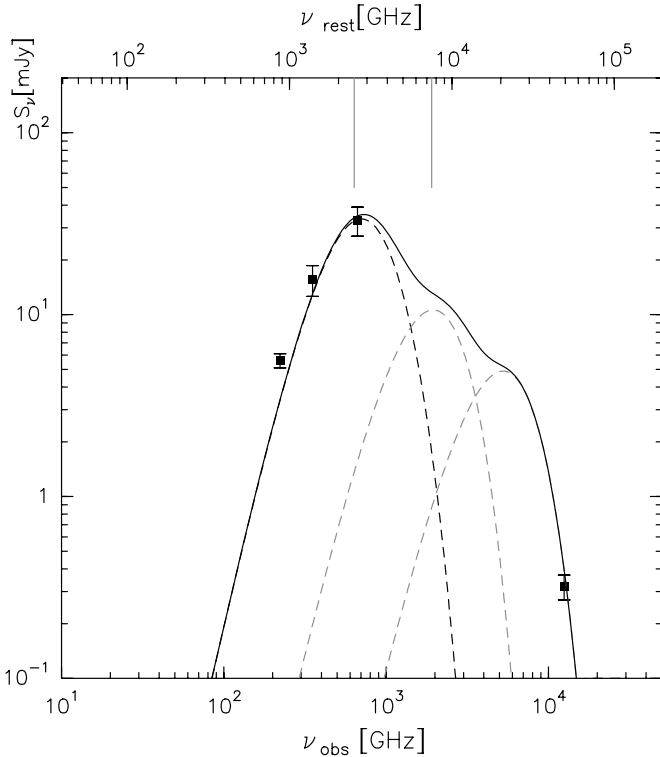


Figure 3. Dust SED toward SMM J14009+0252. The black and the two gray dotted lines show a 40, 75, and 200 K dust component, respectively. The far-IR luminosity of this model is $3.8 \times 10^{12} L_{\odot}$. The solid gray lines at the top indicate the rest-frame 40–120 μm integration limits used to compute the far-IR luminosity.

SMM J14009+0252. The observed CO(5–4) to CO(3–2) line ratio (0.7) implies that the CO emission is sub-thermally excited, at least for the CO(5–4) line. This line ratio is identical to that observed for SMM J16359+6612 (Weiß et al. 2005) and we employ the large velocity gradient models discussed in that paper to estimate a CO(1–0) line luminosity of $L' \approx 8.2 \times 10^{10}$ K km s⁻¹ pc². This translates into a molecular gas mass of $M_{\text{H}_2} \approx 6.5 \times 10^{10} M_{\odot}$ using a standard ULIRG conversion factor of $0.8 M_{\odot} (\text{K km s}^{-1} \text{pc}^2)^{-1}$ (Downes & Solomon 1998). These numbers take the lens magnification of $m = 1.5$ due to the foreground cluster, Abell 1835 at $z = 0.25$, into account (Ivison et al. 2000).

The large molecular gas mass is in line with estimates based on the dust continuum measurements. The 1350, 850, and 450 μm observations (see Ivison et al. 2000, for a compilation of the observed flux densities) can be described by a dust temperature of $\sim 40\text{K}$ (similar to the kinetic temperature of the CO model) and a gas mass of $M_{\text{H}_2} \approx 8 \times 10^{10} M_{\odot}$ using the

dust model in Weiß et al. (2007) and a gas-to-dust mass ratio of 100. The implied far-IR luminosity (integral between 40 and 120 μm , Helou et al. 1985) of this model is $\approx 3 \times 10^{12} L_{\odot}$, which corresponds to a star formation rate of $\approx 500 M_{\odot} \text{yr}^{-1}$. These numbers classify SMM J14009+0252 as a ULIRG.

We note, however, that this model underestimates the observed 24 μm flux density and additional warmer dust components are required to fit the mid-IR data (see Figure 3). Such a multi-component dust model predicts $L_{\text{FIR}} \approx 4\text{--}5 \times 10^{12} L_{\odot}$, although the lack of data between 24 μm and 450 μm means that the shape of the Wien tail of the dust SED is not well constrained. In any case, the estimated far-IR luminosity is far ($\sim \times 5$) lower than estimates based on the radio/far-IR correlation (Condon 1992) which supports the conclusion of Ivison et al. (2000) that SMM J14009+0252 contains a radio-loud active galactic nucleus.

We thank the IRAM telescope operators for their support during the observations. IRAM is supported by INSU/CNRS (France), MPG (Germany), and IGN (Spain).

REFERENCES

- Barger, A. J., Cowie, L. L., & Sanders, D. B. 1999, *ApJ*, **518**, 5
 Borys, C., Chapman, S. C., Halpern, M., & Scott, D. 2003, *MNRAS*, **334**, 385
 Chapman, S. C., Blain, A. W., Smail, I., & Ivison, R. J. 2005, *ApJ*, **622**, 772
 Condon, J. J. 1992, *ARA&A*, **30**, 575
 Coppin, K., et al. 2006, *MNRAS*, **372**, 1621
 Dannerbauer, H., Lehnert, M. D., Lutz, D., Tacconi, L., Bertoldi, F., Carilli, C., Genzel, R., & Menten, K. 2002, *ApJ*, **573**, 473
 Downes, D., & Solomon, P. M. 1998, *ApJ*, **507**, 615
 Erickson, N., Narayanan, G., Goeller, R., & Grosslein, R. 2007, in ASP Conf. Ser. 375, From Z-Machines to ALMA: (Sub)Millimeter Spectroscopy of Galaxies, ed. A. J. Baker, J. Glenn, A. I. Harris, J. G. Mangum, & M. S. Yun (San Francisco, CA: ASP), 71
 Greve, T. R., et al. 2004, *MNRAS*, **354**, 779
 Harris, A. I., et al. 2007, in ASP Conf. Ser. 375, From Z-Machines to ALMA: (Sub)Millimeter Spectroscopy of Galaxies, ed. A. J. Baker, J. Glenn, A. I. Harris, J. G. Mangum, & M. S. Yun (San Francisco, CA: ASP), 82
 Helou, G., Soifer, B. T., & Rowan-Robinson, M. 1985, *ApJ*, **298**, 7
 Hempel, A., Schaerer, D., Egami, E., Pelló, R., Wise, M., Richard, J., Le Borgne, J. F., & Kneib, J. P. 2008, *A&A*, **477**, 55
 Ivison, R. J., Smail, I., Barger, A. J., Kneib, J.-P., Blain, A. W., Owen, F. N., Kerr, T. H., & Cowie, L. L. 2000, *MNRAS*, **315**, 209
 Ivison, R. J., et al. 2002, *MNRAS*, **337**, 1
 Ivison, R. J., et al. 2004, *ApJS*, **154**, 124
 Naylor, B. J., et al. 2003, *Proc. SPIE*, **4855**, 239
 Smail, I., Ivison, R. J., & Blain, A. W. 1997, *ApJ*, **490**, 5
 Smail, I., Ivison, R. J., Blain, A. W., & Kneib, J. P. 2002, *MNRAS*, **331**, 495
 Spergel, D. N., et al. 2003, *ApJS*, **148**, 175
 Weiß, A., Downes, D., Neri, R., Walter, F., Henkel, C., Wilner, D. J., Wagg, J., & Wiklind, T. 2007, *A&A*, **467**, 955
 Weiß, A., Downes, D., Walter, F., & Henkel, C. 2005, *A&A*, **440**, 45
 Yun, M. S., & Carilli, C. L. 2002, *ApJ*, **568**, 88